AGU PUBLICATIONS

Geophysical Research Letters

RESEARCH LETTER
10.1002/2017GL073593

Key Points:
- Eddy covariance measurements of air-sea gas transfer velocity from an icebreaker in open-water and sea ice regions of the eastern Arctic
- Open-water measurements in agreement with bulk parameterizations
- Air-sea gas transfer velocity has a near-linear dependence on decreasing sea ice concentration

Supporting Information:
- Supporting Information S1

Correspondence to:
J. Prytherch,
earjpr@leeds.ac.uk

Citation:
Prytherch, J., I. M. Brooks, P. M. Crill, B. F. Thornton, D. J. Salisbury, M. Tjernström, L. G. Anderson, M. C. Geibel, and C. Humborg (2017), Direct determination of the air-sea CO_2 gas transfer velocity in Arctic sea ice regions, *Geophys. Res. Lett.*, *44*, 3770–3778, doi:10.1002/2017GL073593.

Received 6 JAN 2017
Accepted 29 MAR 2017
Accepted article online 3 APR 2017
Published online 24 APR 2017

Direct determination of the air-sea CO_2 gas transfer velocity in Arctic sea ice regions

John Prytherch[1,2], Ian M. Brooks[1], Patrick M. Crill[3], Brett F. Thornton[3], Dominic J. Salisbury[1], Michael Tjernström[2], Leif G. Anderson[4], Marc C. Geibel[5], and Christoph Humborg[6]

[1]School of Earth and Environment, University of Leeds, Leeds, UK, [2]Department of Meteorology and Bolin Centre for Climate Research, Stockholm, Sweden, [3]Department of Geological Sciences, Stockholm University, Stockholm, Sweden, [4]Department of Marine Sciences, University of Gothenburg, Gothenburg, Sweden, [5]Baltic Sea Centre, Stockholm University, Stockholm, Sweden, [6]Department of Environmental Science and Analytical Chemistry, Stockholm University, Stockholm, Sweden

Abstract The Arctic Ocean is an important sink for atmospheric CO_2. The impact of decreasing sea ice extent and expanding marginal ice zones on Arctic air-sea CO_2 exchange depends on the rate of gas transfer in the presence of sea ice. Sea ice acts to limit air-sea gas exchange by reducing contact between air and water but is also hypothesized to enhance gas transfer rates across surrounding open-water surfaces through physical processes such as increased surface-ocean turbulence from ice-water shear and ice-edge form drag. Here we present the first direct determination of the CO_2 air-sea gas transfer velocity in a wide range of Arctic sea ice conditions. We show that the gas transfer velocity increases near linearly with decreasing sea ice concentration. We also show that previous modeling approaches overestimate gas transfer rates in sea ice regions.

1. Introduction

1.1. Arctic Ocean CO_2 Uptake

In the Arctic Ocean, cooling waters in wintertime act to increase CO_2 solubility, enhancing uptake from the atmosphere, while formation of sea ice promotes deepwater formation, sequestering CO_2 from surface waters into the deep ocean. In summertime, primary production acts to draw down CO_2. These processes combine for an estimated net air-sea flux of −66 to −199 Tg C yr^{-1} into the Arctic Ocean [*Bates and Mathis*, 2009], 4% to 12% of the net global oceanic CO_2 uptake [*Takahashi et al.*, 2009]. Sea ice is also known to be permeable to gases [*Miller et al.*, 2011] and may act both as a sink for CO_2 during melt [*Delille et al.*, 2014] and a source of CO_2 during freezeup conditions [*Delille et al.*, 2007]. When melt ponds form on the sea ice, they may act as an additional sink due to the initially low CO_2 concentration in the meltwater [*Geilfus et al.*, 2015].

The Arctic is undergoing accelerating ice loss and a widening of the summertime marginal ice zone (MIZ: a region with sea ice concentration between 15% and 80% adjoining both pack ice and sparse ice), with the poleward expansion of the MIZ outpacing the contraction of the equatorward edge [*Strong and Rigor*, 2013]. Ice cover and thickness are also reducing substantially in the central Arctic, with a decrease in annual mean thickness from 3.59 m to 1.25 m between 1975 and 2012 [*Lindsay and Schweiger*, 2015]. The impact of reduced sea ice cover on the Arctic CO_2 sink is complex and poorly understood [*Parmentier et al.*, 2013], with both increases [*Arrigo et al.*, 2008] and decreases [*Cai et al.*, 2010] in the magnitude of the sink predicted.

1.2. Gas Transfer Velocity

The flux of a poorly soluble trace gas, such as CO_2, across the air-water interface, F_{CO2}, can be represented as a product of the air-water partial-pressure difference, ΔpCO_2; the aqueous-phase solubility of the gas, K_0; and an exchange rate, or transfer velocity, k:

$$F_{CO2} = kK_0\ \Delta pCO_2 \quad (1)$$

The uncertainty in the magnitude of the current and future Arctic CO_2 sink critically depends on poor understanding of k in the presence of sea ice. Other sources of uncertainty include the difficulty in estimating the

strength and timing of factors which impact waterside CO_2 partial pressure, pCO_{2w}, such as biological export, and the amount of sea ice decline expected in coming years.

The transfer velocity is the kinetic driver of the exchange and represents interfacial turbulent processes that are challenging to measure directly [e.g., *Jähne et al.*, 1987; *McGillis et al.*, 2001; *Wanninkhof et al.*, 2009]. It is typically parameterized in terms of more easily measurable quantities, most commonly wind speed, the primary driver of ocean near-surface turbulence.

To estimate k_{eff}, the gas transfer rate in the presence of sea ice, assessments of the polar CO_2 sink have typically used open-water k parameterizations and hypothesized a linear scaling against the fraction of open water, f [e.g., *Takahashi et al.*, 2009]. There are few reported measurements of k_{eff} in sea ice regions. The first used an indirect radon isotope-deficit method [*Fanning and Torres*, 1991]. In ice concentrations greater than 70%, k_{eff} was found to be an order of magnitude higher than expected from a linear scaling. More recent radon isotope-deficit results found k_{eff} suppressed relative to linear scaling for ice concentrations of 56% to 75% [*Rutgers van der Loeff et al.*, 2014]. Indirect estimates [*Loose and Schlosser*, 2011; *Loose et al.*, 2014] and laboratory studies [*Loose et al.*, 2009; *Lovely et al.*, 2015] found that k_{eff} depended on other interfacial turbulence forcing such as shear between floating ice and the underlying water and form drag on the wind from ice edges, in addition to wind speed and f. All these physical processes have been incorporated into a gas transfer model that predicts enhanced transfer rates in the presence of sea ice [*Loose et al.*, 2014].

Measurement of F_{CO2} using eddy covariance (EC) enables k_{eff} to be directly determined from ((1)) and related to forcing conditions on short time scales of 10 min to 1 h and spatial scales on the order of 1 km. In contrast, the radon isotope-deficit method averaging times and spatial scales are on the order of 3.5 days and 20 km, much longer than the periods over which local forcing changes with the movement of weather systems.

A large disparity exists in reported EC CO_2 fluxes in sea ice regions. Several experiments have reported highly variable fluxes, including measurements higher than typical open ocean values by an order of magnitude or more [*Zemmelink et al.*, 2006; *Else et al.*, 2011; *Miller et al.*, 2011; *Papakyriakou and Miller*, 2011; *Sørensen et al.*, 2014; *Sievers et al.*, 2015]. However, the open-path CO_2 flux instrumentation used in these studies is now known to be unsuitable for marine measurement: optical contamination and water vapor cross sensitivity [*Miller et al.*, 2010; *Blomquist et al.*, 2014] result in large biases [*Prytherch et al.*, 2010] which are not correctable [*Landwehr et al.*, 2014]. Other studies have reported similarly large fluxes in Pacific and Siberian sectors of the Arctic [*Semiletov et al.*, 2004; *Semiletov et al.*, 2007], but details of the flux measurements are not available. Experiments using closed-path instrumentation [*Sievers et al.*, 2015] or different methods such as chamber flux measurements [*Geilfus et al.*, 2012; *Nomura et al.*, 2013; *Delille et al.*, 2014; *Geilfus et al.*, 2015] report much smaller fluxes. The EC and chamber flux experiments listed did not determine k_{eff}. Recent extensive measurements from an automated closed-path EC flux system on an icebreaker operating in the Southern Ocean indicate a linear dependence of k_{eff} on f [*Butterworth and Miller*, 2016a].

Here we report the first direct determination of CO_2 gas transfer velocity obtained in the Arctic MIZ, as well as in pack ice and open water. Observations were made in the eastern Arctic Ocean shelf region from the Swedish icebreaker *Oden* during the 3 month Arctic Clouds in Summer Experiment (ACSE), a component of the Swedish-Russian-US Arctic Ocean Investigation on Climate-Cryosphere-Carbon Interactions (SWERUS-C3). An analysis of measurements in both open water and variable sea ice conditions is used to evaluate models of gas exchange in sea ice.

2. Methods

2.1. Expedition

The primary purpose of ACSE was to study Arctic clouds, their effect on the surface energy balance and hence sea ice, and the effect of surface conditions on cloud properties during the summer melt and early autumn freezeup [*Sotiropoulou et al.*, 2016]. A primary goal of SWERUS-C3 was to study the Arctic Ocean carbon cycles, and the results presented here are the result of an ad hoc collaboration during the expedition. The expedition began in Tromsø, Norway, on 5 July 2014, day of year 186 (DOY; defined as 1.0 at 00 UTC on 1 January; all times given in UTC). The ship crossed the Kara, Laptev, East Siberian, and Chukchi Seas, mostly on or just off the edge of the Siberian shelf, arriving in Barrow, Alaska, on 19 August (DOY 231). A second leg started on 20 August and returned to Tromsø, via a route somewhat farther north, ending on 5

October (DOY 278; Figure S1 in the supporting information). An extensive suite of in situ and remote sensing instrumentation was installed on *Oden* [*Tjernström et al.*, 2015; *Achtert et al.*, 2015], of which only that relevant to the observations reported here is described below.

2.2. Measurements

The three-dimensional wind vector and CO_2 mixing ratio were determined at 10 Hz by a sonic anemometer mounted on a mast installed over *Oden*'s bow and a Los Gatos Research Fast Greenhouse Gas Analyzer (FGGA) at the base of the mast, with an inlet co-located with the anemometer. The FGGA measures humidity and controls temperature and pressure within its measurement volume to obtain CO_2 dry mole fraction [*Baer et al.*, 2002; *Yang et al.*, 2016], and additional correction for dilution effects is not required. An inline drier, such as a Nafion system, may reduce noise in the dry mole fraction calculation and is recommended for closed-path marine flux measurement [*Miller et al.*, 2010; *Blomquist et al.*, 2014; *Butterworth and Miller*, 2016b] but was not available here. Additional information on the instrumentation and data processing, including corrections for platform motion and airflow distortion, is given in the supporting information but follows well-established methods [*Edson et al.*, 1998; *Prytherch et al.*, 2015]. EC CO_2 fluxes were determined over 20 min long averaging intervals. Mean winds were adjusted to a standard 10 m reference height and neutral stability (U_{10n}) by using the Businger-Dyer relationships [*Businger*, 1988]. The solubility of CO_2 in seawater was determined following *Weiss* [1974] by using water temperature and salinity measured continuously at 1 Hz with a Seabird TSG mounted on the *Oden*'s underway sample line with an inlet at 8 m depth. During the expedition's first leg, pCO_{2w} was measured continuously by using the Stockholm University Water Equilibration Gas Analyser System (WEGAS) [*Thornton et al.*, 2016], sampling from the ship's underway sampling line. Closest-to-surface water samples from conductivity-temperature-depth (CTD) rosette bottles at 5 to 10 m depth were also used to measure pCO_{2w} at stations during the expedition (Figure 1). The ΔpCO_2 was determined preferentially from the WEGAS system and the FGGA mast measurements. When the WEGAS system was unavailable, bottle measurements were linearly interpolated to the flux-observation time with a maximum allowed time difference of 12 h. The root-mean-square error in the transfer velocity resulting from ΔpCO_2 uncertainty is estimated to be 17%. Gas transfer velocity was calculated from ((1)) and normalized to a Schmidt number of 660 with an exponent of 0.5 following *Wanninkhof* [2014]. Further details on the ΔpCO_2 uncertainty and transfer velocity calculation are provided in the supporting information.

From the 3 months of the expedition, there were 1146 20 min flux-observation periods with all the necessary data to determine transfer velocities, acceptable relative wind directions (±120° from the bow) and minimal ship maneuvering. Of these, 953 were determined to have turbulent statistics that passed quality control measures for flux calculations, following *Foken and Wichura* [1996]. The CO_2 flux measurement uncertainty was determined following the approach of *Blomquist et al.* [2014]; further information is provided in the supporting information. For a wind speed of 7 m s^{-1}, the ΔpCO_2 at which 20 min CO_2 flux uncertainty was 100% was ~40 ppm (Figure S2). This was set as the minimum threshold, a criteria met by 734 periods.

Sea ice concentration is obtained from Advanced Microwave Scanning Radiometer 2 (AMSR2) satellite passive microwave measurements [*Spreen et al.*, 2008] by using the Artist sea ice algorithm (ASI 5). Daily concentration estimates on a 6.25 km grid are obtained from the University of Bremen (http://www.iup.uni-bremen.de:8084/amsr2/#Arctic). Flux measurements were matched to the grid cell containing Oden's position, and the ice concentration measurement interpolated to the flux measurement time.

There are 277 measurements classified as open water (ice concentration less than 1%). Following removal of outliers (more than two standard deviations from the mean), 263 open-water measurements are included in this analysis. For analysis of measurements in sea ice, the ratio $k_{eff}/k_{Wan'14}$, where $k_{Wan'14}$ is a quadratic wind speed-dependent open ocean estimate [*Wanninkhof*, 2014], is used to remove the wind speed dependence of k_{eff}. Measurements for which the absolute value of this ratio was greater than 10 were removed, prior to removal of outliers as defined above.

3. Results

EC gas flux measurements were obtained in and close to sea ice during both the summer melt season and the beginning of the autumn freezeup (Figures 1 and S1). For the ACSE measurements, these seasons are defined as DOY 186 to 239.5 and DOY 239.5 to 275, respectively [*Sotiropoulou et al.*, 2016], with CO_2 flux

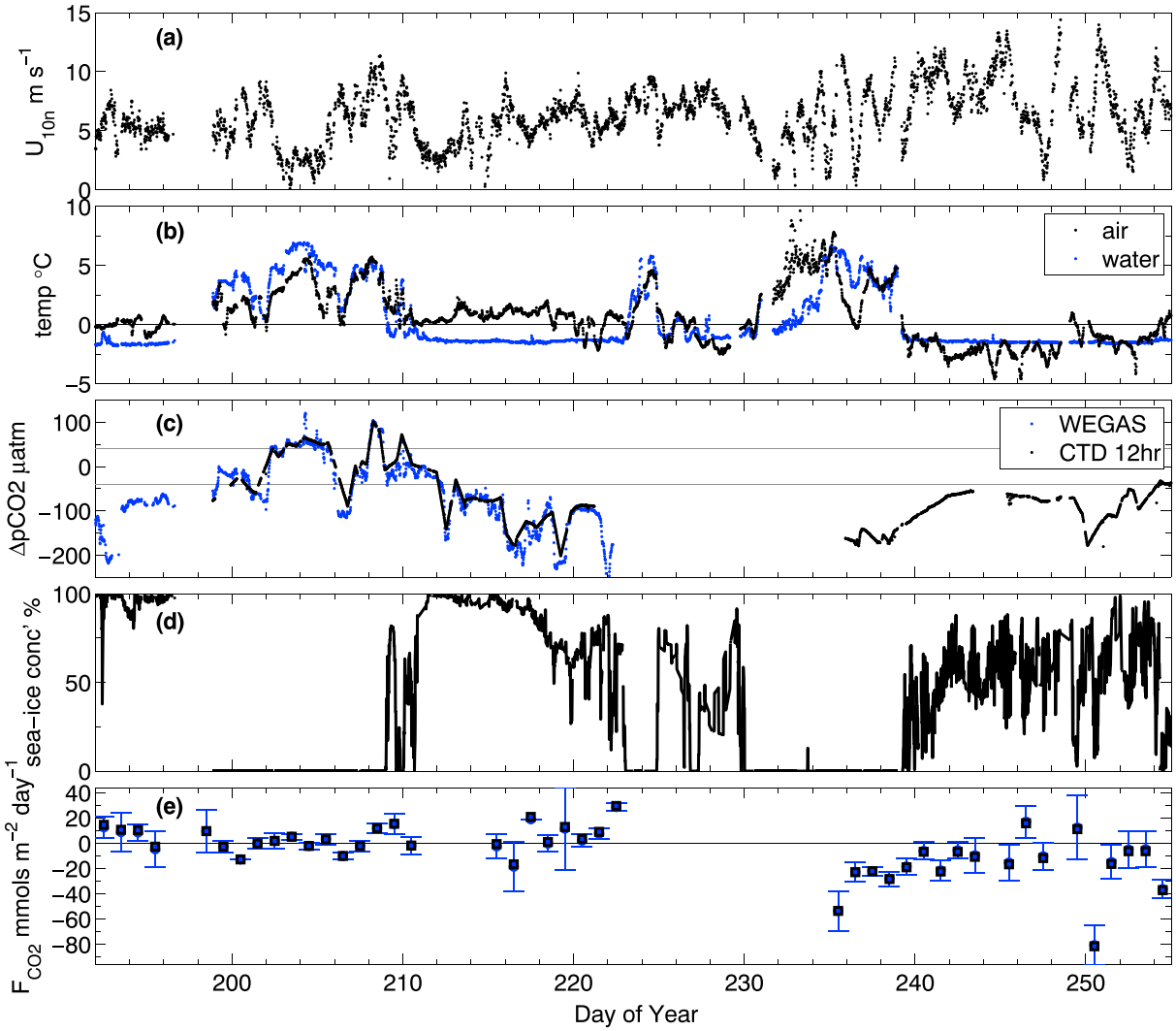

Figure 1. Environmental conditions during the ACSE expedition. (a) U_{10n} determined from sonic anemometer measurements. (b) 10 m air temperature, and 8 m depth water temperature. (c) Sea-air ΔpCO_2 determined from airside FGGA measurements and waterside measurements from either the WEGAS underway system or CTD samples at between 5 and 10 m depth. The grey lines show ±40 µatm. (d) Sea ice concentration from daily AMSR2 ASI 5 maps. (e) Daily mean CO_2 flux measurements. The error bars show standard error, and the black boxes show removal of sea ice and melt pond fluxes.

measurements made between DOY 192 and 255. During the summer season, winds were light to moderate, with the 20 min vector average U_{10n} varying from 0.9 to 11.3 m s^{-1} (mean 6.6 ± 2.0 m s^{-1}, where the variability is 1 standard deviation unless otherwise stated). Winds during autumn were slightly higher (mean 7.4 m s^{-1} ± 2.4 m s^{-1}). From DOY 197 to DOY 209, the *Oden* was operating in open water, transiting through the east Arctic from 125.5°E to 175.6°E at latitudes between 74.2°N and 79.4°N. During this period ΔpCO_2 was relatively small (1 ± 57 µatm) and varied between positive and negative. Flux measurements were made from *Oden* in sea ice during 14 days in summer. Sea ice concentration was consistently above 80% with melt ponds present, and large negative ΔpCO_2 (−126 ± 48 µatm). During the autumn freezeup, *Oden* transited from 174°W to 142°E at latitudes between 72.1°N and 81.4°N. Sea ice was more variable, melt ponds were no longer present, and sea ice conditions included grease and pancake ice. For the 14 days that *Oden* was in sea ice in autumn and flux measurements were made, the ΔpCO_2 gradient remained strongly negative (−88 ± 25 µatm). The variability in ΔpCO_2 during the expedition was primarily spatial rather than temporal (Figure S1). Overall, 340 of 541 flux measurements >5 mmol m^{-2} d^{-1} were in the direction expected from the measured ΔpCO_2. Measurements in the opposite direction to that expected may result from natural variability in a stochastic process, measurement error, or environmental factors, discussed below.

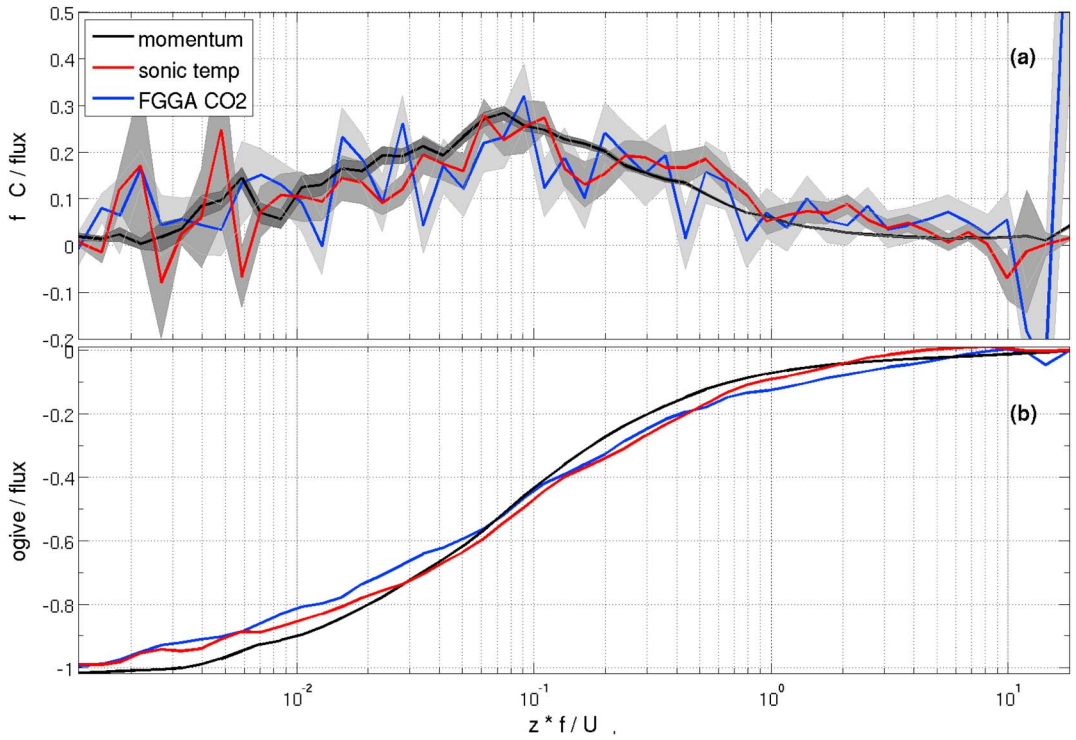

Figure 2. Momentum, sonic temperature, and CO_2 (a) flux cospectra and (b) ogives, normalized by the flux. Cospectra shown are an average of 88 20 min records, with sea ice concentration of <1%, U_{10n} between 4 and 7 m s^{-1} and $|\Delta pCO_2| > 40$ ppm. The shaded areas show standard error. Frequency is normalized by using measurement height z and relative wind speed U_{rel} in order to remove wind speed dependence.

CO_2 cospectra and cospectral ogives are more variable than those for the momentum and sonic temperature flux measurements (Figure 2), reflecting the higher measurement noise, though all have the expected shape. Open-water k measurements are in good agreement with bulk wind speed-dependent parameterizations (Figure 3). The wind speed-binned measurements, excluding the highest wind bin (consisting of two measurements), are best fit by a quadratic wind speed relationship (r^2 0.97), and the bulk quadratic [*Wanninkhof*, 2014] parameterization falls within the standard error of the binned measurement means.

Measured k_{eff} in sea ice regions has a close-to-linear dependence on f (Figure 4) when normalized by the *Wanninkhof* [2014] parameterization, $k_{Wan'14}$, to remove the wind speed dependence. Distributions of $k_{eff}/k_{Wan'14}$ within each 25% wide ice-concentration bin are approximately normal, and hence, means and medians from each bin are similar. The mean remains above zero for all ice concentrations. The mean range of these measurements encompasses a previous estimate of k_{eff} derived from radon isotope-deficit-derived measurements [*Rutgers van der Loeff et al.*, 2014].

4. Discussion

Error in the determination of ΔpCO_2 results from temporal and spatial variabilities of pCO_{2w} (see the supporting information) and may also be introduced by vertical near-surface pCO_{2w} gradients. Surface pCO_{2w} may be higher than at 8 m depth when fluxes are into the water, causing our estimates of k_{eff} to be biased low. Wind, ice-water shear, and convection all act to mix surface water, even in near-100% sea ice or low-wind conditions [e.g., *Sirevaag et al.*, 2011], and temperature profiles from CTD stations showed a well-mixed layer to depths below 10 m throughout the expedition. Convection-induced mixing in autumn would act to reduce any vertical pCO_{2w} gradient. No statistically significant difference (using two-sample t and Wilcoxon rank sum tests at the 10% level) was found between sea ice-binned k_{eff} measured in summer and in autumn, suggesting that any net effect from vertical pCO_{2w} gradients was small.

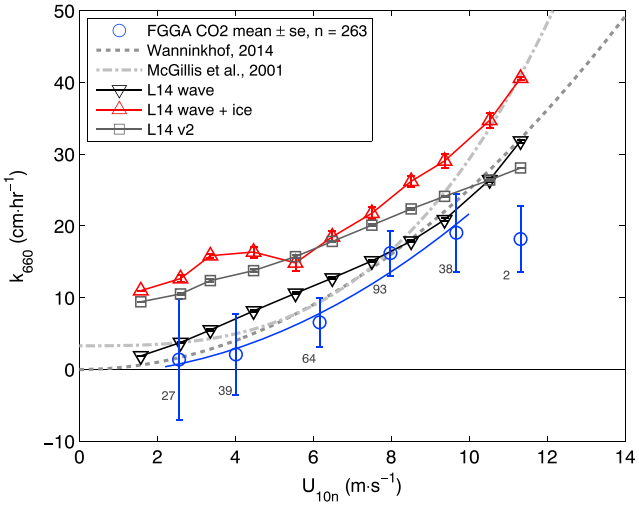

Figure 3. Open-water (sea ice concentration $< 1\%$) k. FGGA CO_2 measurements are binned in 2 m s^{-1} wide wind speed bins (blue circles), with the number of measurements within each bin shown. A quadratic fit to the binned measurements between 1 and 11 m s^{-1}, quadratic and cubic wind speed-based bulk parameterizations, the L14 model wave, wave plus ice terms, and L14 v2 model are also shown.

The measured CO_2 flux, F_{meas}, incorporates contributions from sea ice, F_{ice}, and from melt ponds on sea ice, F_{mp}, as well as from F_{CO2}:

$$F_{meas} = (1 - f - f_{mp})F_{ice} + (f_{mp})F_{mp} + (f)F_{CO2} \quad (2)$$

where f_{mp} is the fractional coverage of melt ponds. Here we assess the potential bias resulting from ice and melt pond contributions to the total flux. We estimate F_{ice} as ±2 mmol m^{-2} d^{-1}, the mean of fluxes measured in near-freezing conditions [*Delille et al.*, 2014]. We assume that ice acts as a sink during the summer melt [*Delille et al.*, 2014] and as a source during the autumn freezeup [*Delille et al.*, 2007]. Following their formation, which typically occurs in June, melt ponds rapidly reach near equilibrium with atmospheric pCO_2. A small sink of approximately -1 mmol m^{-2} d^{-1} is maintained due to continued replenishment of the low pCO_{2w}

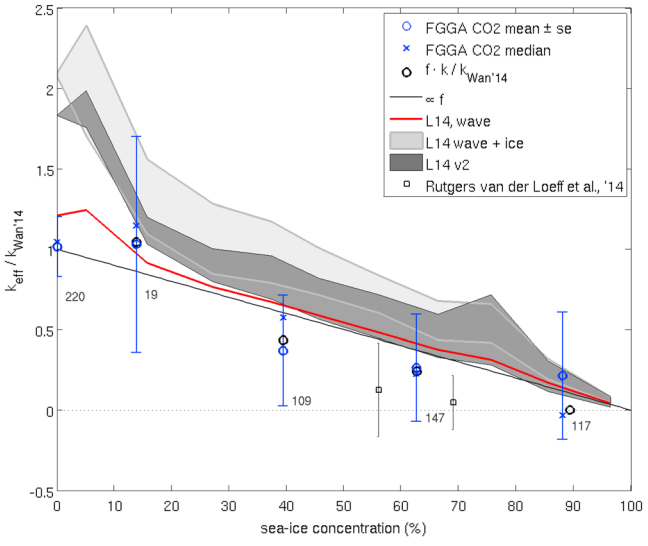

Figure 4. FGGA CO_2 k_{eff} normalized by $k_{Wan'14}$ and means binned by AMSR2 ASI 5 sea ice concentration (bin boundaries at 0%, 1%, 25%, 50%, 75%, and 100%). Median bin values and the number of measurements in each bin are also shown. The L14 model wave and wave plus ice terms, and the L14 v2 model are shown. The shaded regions represent ice-water relative velocity, V_{ice}, of 0 to 0.2 m s^{-1}. Also shown are radon-deficit-derived k_{eff} [*Rutgers van der Loeff et al.*, 2014], scaled k, the transfer velocity from F_{CO2} only (equation (2)) and the linear scaling of $k_{eff}/k_{Wan'14}$ with fraction of open water, f.

meltwater [*Geilfus et al.*, 2015; *Nomura et al.*, 2013; *Geilfus et al.*, 2012]. We apply this estimate of F_{mp} to a melt pond period, defined as up until DOY 218. After this time, ponds were observed to have generally melted through to the underlying seawater [*Tjernström et al.*, 2015]. Melt ponds are not distinguished from open water in the AMSR2 retrieval [*Kern et al.*, 2016]; we assume that in sea ice, $f_{mp} = 0.5\ f$, with f then reduced accordingly.

In sea ice concentration >25%, the area-weighted CO_2 flux from sea ice (mean = 0.14 mmol m^{-2} d^{-1}, absolute mean = 1.27 mmol m^{-2} d^{-1}) and CO_2 flux from melt ponds during the melt pond period (mean = −0.02 mmol m^{-2} d^{-1}) are small relative to the measured flux (mean = −7.82 mmol m^{-2} d^{-1}, absolute mean = 35.26 mmol m^{-2} d^{-1}). The transfer velocity determined from only F_{CO2} (equations (1) and (2)) and scaled by f is well within the range of k_{eff} in each sea ice bin (Figure 4). For ice concentrations >75%, removal of sea ice and melt pond fluxes has the greatest effect, reducing the transfer rate from above the linear scaling to near zero.

The model of air-sea gas exchange developed by *Loose et al.* [2014, hereafter L14] predicts enhanced gas transfer in the presence of sea ice. The model produces separate estimates of gas transfer due to the action of short waves in open water and leads [*Frew et al.*, 2004], and the competing influences of shear (the sum of contributions from the air-sea interface, ice-water interface, and form drag from ice edges) and buoyancy forcing, collectively termed "ice effects" in the model. The wave and ice terms cannot strictly be summed to obtain a single estimate of k_{eff} due to similarity considerations (B. Loose, personal communication). The velocity of ice relative to the underlying water, V_{ice}, was not measured during ACSE; an estimated V_{ice} from 0 to 0.2 m s^{-1} was chosen as a representative range of Arctic ice drift velocities [*Hakkinen et al.*, 2008]. The L14 model forced with observations of wind speed, sea ice concentration, and air and water temperature predicts enhanced gas transfer in sea ice. The wave term alone predicts k_{eff} greater than a linear scaling with f (Figure 4). While an unaccounted for surface gradient in pCO_{2w} could cause a low bias in our k_{eff} measurements, such a gradient would itself be reduced by enhanced waterside turbulence.

The L14 model is not specifically designed for open water. During ACSE open-water conditions were marginally convective (mean water-air temperature difference 1.1°C; Figure 1). The buoyancy component of the L14 model ice term, nonzero when water temperature is greater than air, results in overestimation of k at wind speeds below 11 m s^{-1} (Figure 3). Removal of the buoyancy-driven component of the model when $f = 1$ reduces the L14 ice term to zero, improving agreement with observations.

A recent development of the L14 model, here termed L14 v2 (https://github.com/bloose/keff_in_SealceZone.git; B. Loose, personal communication), relates wind speed, wave breaking, and turbulent dissipation by using field measurements [*Sutherland and Melville*, 2015; *Smith and Thomson*, 2016; *Zippel and Thomson*, 2016]. The L14 v2 model produces a single combined estimate of k_{eff}. Forced with ACSE observations and the estimated range of V_{ice}, the L14 v2, estimates of k_{eff} are within the observational standard error range in sea ice conditions (Figure 4).

5. Conclusions

We report direct EC determinations of CO_2 k_{eff} in open water, marginal sea ice, and dense pack ice regions of the Arctic. In open water, the measurements have a quadratic dependence on wind speed and are in good agreement with previously published parameterizations. In sea ice, the measurements show an approximately linear dependence of k_{eff} on f. Due to the large ΔpCO_2 during the experiment, estimated fluxes from sea ice and melt ponds were a small fraction of the total measured CO_2 flux and acted to reduce k_{eff} at high ice concentrations. The eddy covariance measurements in sea ice are highly variable as a result of the measurement uncertainty inherent in both a ship-based EC trace gas measurement and in the ΔpCO_2 within the flux footprint. The range of these results encompasses both indirect estimates of k_{eff} from radon-deficit experiments in the Arctic [*Rutgers van der Loeff et al.*, 2014], and recent direct k_{eff} measurements obtained in the Antarctic MIZ and Southern Ocean [*Butterworth and Miller*, 2016a]. The agreement of the only two published sets of EC k_{eff} measurements provides confidence in the utility of this approach.

The L14 model of air-sea-ice gas transfer overestimates k_{eff} when driven by the observed environmental conditions. However, the unpublished L14 v2 model estimates of k_{eff} are largely within the uncertainty

range of the observations. A hypothesized net enhancement of gas transfer due to additional waterside turbulent forcing in the presence of sea ice is not observed in our measurements.

Future field experiments should ideally include additional measurements of ice properties, in situ measurements of V_{ice} and pCO_{2w} within the flux footprint. Measurements of surface pCO_{2w} and near-surface gradients would be of particular value. In the absence of these measurements, our results combined with the EC measurements from the Antarctic MIZ [*Butterworth and Miller*, 2016a] suggest that a linear scaling of k with f [e.g., *Takahashi et al.*, 2009] is the appropriate choice for parameterization of air-sea gas flux in ice-covered polar regions.

Acknowledgments
ACSE was supported by funding from the Knut and Alice Wallenberg Foundation, Swedish Research Council, Faculty of Science at Stockholm University, U.S. Office of Naval Research, the U.S. National Oceanic and Atmospheric Administration (NOAA), and the UK Natural Environment Research Council (grant NE/K011820/1). We are grateful to the Swedish Polar Research Secretariat and to the two captains and crews of the *Oden* for logistics support. All data from ACSE will be made available through the Bolin Centre for Climate Research database (http://www.bolin.su.se).

References

Achtert, P., I. M. Brooks, B. J. Brooks, B. I. Moat, J. Prytherch, P. O. G. Persson, and M. Tjernström (2015), Measurement of wind profiles by motion-stabilised ship-borne Doppler lidar, *Atmos. Meas. Tech.*, *8*(11), 4993–5007, doi:10.5194/amt-8-4993-2015.

Arrigo, K. R., G. van Dijken, and S. Pabi (2008), Impact of a shrinking Arctic ice cover on marine primary production, *Geophys. Res. Lett.*, *35*, L19603, doi:10.1029/2008GL035028.

Baer, D. S., J. B. Paul, M. Gupta, and A. O'Keefe (2002), Sensitive absorption measurements in the near-infrared region using off-axis integrated cavity output spectroscopy, in *International Symposium on Optical Science and Technology*, pp. 167–176, Int. Soc. for Opt. and Photonics, Seattle, Wash., doi:10.1117/12.451461.

Bates, N. R., and J. T. Mathis (2009), The Arctic Ocean marine carbon cycle: Evaluation of air-sea CO_2 exchanges, ocean acidification impacts and potential feedbacks, *Biogeosciences*, *6*(11), 2433–2459.

Blomquist, B. W., B. J. Huebert, C. W. Fairall, L. Bariteau, J. B. Edson, J. E. Hare, and W. R. McGillis (2014), Advances in air-sea CO_2 flux measurement by eddy correlation, *Boundary Layer Meteorol.*, *152*(3), 245–276, doi:10.1007/s10546-014-9926-2.

Businger, J. A. (1988), A note on the Businger-Dyer profiles, *Boundary Layer Meteorol.*, *42*, 145–151, doi:10.1007/978-94-009-2935-7_11.

Butterworth, B. J., and S. D. Miller (2016a), Air-sea exchange of carbon dioxide in the Southern Ocean and Antarctic marginal ice zone, *Geophys. Res. Lett.*, *43*, 7223–7723, doi:10.1002/2016GL069581.

Butterworth, B. J., and S. D. Miller (2016b), Automated underway eddy covariance system for air-sea momentum, heat, and CO_2 fluxes in the Southern Ocean, *J. Atmos. Ocean. Technol.*, *33*(4), 635–652.

Cai, W. J., et al. (2010), Decrease in the CO_2 uptake capacity in an ice-free Arctic Ocean basin, *Science*, *329*(5991), 556–559, doi:10.1126/science.1189338.

Delille, B., B. Jourdain, A. V. Borges, J. Tison, and D. Delille (2007), Biogas (CO_2, O_2, dimethylsulfide) dynamics in spring Antarctic fast ice, *Limnol. Oceanogr.*, *52*(4), 1367, doi:10.4319/lo.2007.52.4.1367.

Delille, B., et al. (2014), Southern Ocean CO_2 sink: The contribution of the sea ice, *J. Geophys. Res. Oceans*, *119*, 6340–6355, doi:10.1002/2014JC009941.

Edson, J. B., A. A. Hinton, K. E. Prada, J. E. Hare, and C. W. Fairall (1998), Direct covariance flux estimates from mobile platforms at sea, *J. Atmos. Ocean. Technol.*, *15*(2), 547–562.

Else, B. G. T., T. N. Papakyriakou, R. J. Galley, W. M. Drennan, L. A. Miller, and H. Thomas (2011), Wintertime CO_2 fluxes in an Arctic polynya using eddy covariance: Evidence for enhanced air-sea gas transfer during ice formation, *J. Geophys. Res.*, *116*, C00G03, doi:10.1029/2010JC006760.

Fanning, K. A., and L. M. Torres (1991), ^{222}Rn and ^{226}Ra: Indicators of sea-ice effects on air-sea gas exchange, *Polar Res.*, *10*(1), 51–58.

Foken, T., and B. Wichura (1996), Tools for quality assessment of surface-based flux measurements, *Agric. For. Meteorol.*, *78*(1), 83–105, doi:10.1016/0168-1923(95)02248-1.

Frew, N. M., et al. (2004), Air-sea gas transfer: Its dependence on wind stress, small-scale roughness, and surface films, *J. Geophys. Res.*, *109*, C08S17, doi:10.1029/2003JC002131.

Geilfus, N. X., G. Carnat, T. Papakyriakou, J. L. Tison, B. Else, H. Thomas, E. Shadwick, and B. Delille (2012), Dynamics of pCO_2 and related air-ice CO_2 fluxes in the Arctic coastal zone (Amundsen Gulf, Beaufort Sea), *J. Geophys. Res.*, *117*, C00G10, doi:10.1029/2011JC007118.

Geilfus, N. X., R. J. Galley, O. Crabeck, T. Papakyriakou, J. Landy, J. L. Tison, and S. Rysgaard (2015), Inorganic carbon dynamics of melt-pond-covered first-year sea ice in the Canadian Arctic, *Biogeosciences*, *12*(6), 2047–2061, doi:10.5194/bg-12-2047-2015.

Hakkinen, S., A. Proshutinsky, and I. Ashik (2008), Sea ice drift in the Arctic since the 1950s, *Geophys. Res. Lett.*, *35*, L19704, doi: 10.1029/2008GL034791.

Jähne, B., K. O. Münnich, R. Bösinger, A. Dutzi, W. Huber, and P. Libner (1987), On the parameters influencing air-water gas exchange, *J. Geophys. Res.*, *92*, 1937–1949, doi:10.1029/JC092iC02p01937.

Kern, S., A. Rösel, L. T. Pedersen, N. Ivanova, R. Saldo, and R. T. Tonboe (2016), The impact of melt ponds on summertime microwave brightness temperatures and sea-ice concentrations, *Cryosphere*, *10*(5), 2217, doi:10.5194/tc-10-2217-2016.

Landwehr, S., S. D. Miller, M. J. Smith, E. S. Saltzman, and B. Ward (2014), Analysis of the PKT correction for direct CO_2 flux measurements over the ocean, *Atmos. Chem. Phys.*, *14*(7), 3361–3372, doi:10.5194/acp-14-3361-2014.

Lindsay, R., and A. Schweiger (2015), Arctic sea ice thickness loss determined using subsurface, aircraft, and satellite observations, *Cryosphere*, *9*(1), 269–283, doi:10.5194/tc-9-269-2015.

Loose, B., and P. Schlosser (2011), Sea ice and its effect on CO_2 flux between the atmosphere and the Southern Ocean interior, *J. Geophys. Res.*, *116*, C11019, doi:10.1029/2010JC006509.

Loose, B., W. R. McGillis, P. Schlosser, D. Perovich, and T. Takahashi (2009), Effects of freezing, growth, and ice cover on gas transport processes in laboratory seawater experiments, *Geophys. Res. Lett.*, *36*, L05603, doi:10.1029/2008GL036318.

Loose, B., W. R. McGillis, D. Perovich, C. J. Zappa, and P. Schlosser (2014), A parameter model of gas exchange for the seasonal sea ice zone, *Ocean Sci.*, *10*, 17–28, doi:10.5194/os-10-17-2014.

Lovely, A., B. Loose, P. Schlosser, W. McGillis, C. Zappa, D. Perovich, S. Brown, T. Morell, D. Hsueh, and R. Friedrich (2015), The Gas Transfer through Polar Sea ice experiment: Insights into the rates and pathways that determine geochemical fluxes, *J. Geophys. Res. Oceans*, *120*, 8177–8194, doi:10.1002/2014JC010607.

Lueker, T. J., A. G. Dickson, and C. D. Keeling (2000), Ocean pCO_2 calculated from dissolved inorganic carbon, alkalinity, and equations for K1 and K2: Validation based on laboratory measurements of CO_2 in gas and seawater at equilibrium, *Mar. Chem.*, *70*, 105–119.

McGillis, W. R., J. B. Edson, J. E. Hare, and C. W. Fairall (2001), Direct covariance air-sea CO_2 fluxes, *J. Geophys. Res.*, *106*, 16,729–16,745, doi:10.1029/2000JC000506.

Miller, S. D., C. Marandino, and E. S. Saltzman (2010), Ship-based measurement of air-sea CO_2 exchange by eddy covariance, *J. Geophys. Res.*, *115*, D02304, doi:10.1029/2009JD012193.

Miller, L. A., T. N. Papakyriakou, R. E. Collins, J. W. Deming, J. K. Ehn, R. W. Macdonald, A. Mucci, O. Owens, M. Raudsepp, and N. Sutherland (2011), Carbon dynamics in sea ice: A winter flux time series, *J. Geophys. Res.*, *116*, C02028, doi:10.1029/2009JC006058.

Moat, B. I., M. J. Yelland, and I. M. Brooks (2015), Airflow distortion at instrument sites on the ODEN during the ACSE project, Southampton, GB, National Oceanography Centre, 114 pp., (National Oceanography Centre Internal Document, 17).

Nomura, D., M. A. Granskog, P. Assmy, D. Simizu, and G. Hashida (2013), Arctic and Antarctic sea ice acts as a sink for atmospheric CO_2 during periods of snowmelt and surface flooding, *J. Geophys. Res. Oceans*, *118*, 6511–6524, doi:10.1002/2013JC009048.

Papakyriakou, T., and L. Miller (2011), Springtime CO_2 exchange over seasonal sea ice in the Canadian Arctic Archipelago, *Ann. Glaciol.*, *52*(57), 215–224.

Parmentier, F. J. W., T. R. Christensen, L. L. Sørensen, S. Rysgaard, A. D. McGuire, P. A. Miller, and D. A. Walker (2013), The impact of lower sea-ice extent on Arctic greenhouse-gas exchange, *Nat. Clim. Chang.*, *3*(3), 195–202, doi:10.1038/nclimate1784.

Prytherch, J., M. J. Yelland, R. W. Pascal, B. I. Moat, I. Skjelvan, and C. C. Neill (2010), Direct measurements of the CO_2 flux over the ocean: Development of a novel method, *Geophys. Res. Lett.*, *37*, L03607, doi:10.1029/2009GL041482.

Prytherch, J., M. J. Yelland, I. M. Brooks, D. J. Tupman, R. W. Pascal, B. I. Moat, and S. J. Norris (2015), Motion-correlated flow distortion and wave-induced biases in air-sea flux measurements from ships, *Atmos. Chem. Phys.*, *15*(18), 10,619–10,629, doi:10.5194/acp-15-10619-2015.

Rutgers van der Loeff, M. M., N. Cassar, M. Nicolaus, B. Rabe, and I. Stimac (2014), The influence of sea ice cover on air-sea gas exchange estimated with radon-222 profiles, *J. Geophys. Res. Oceans*, *119*, 2735–2751, doi:10.1002/2013JC009321.

Semiletov, I., A. Makshtas, S. I. Akasofu, and E. Andreas (2004), Atmospheric CO_2 balance: The role of Arctic sea ice, *Geophys. Res. Lett.*, *31*, L05121, doi:10.1029/2003GL017996.

Semiletov, I. P., I. I. Pipko, I. Repina, and N. E. Shakhova (2007), Carbonate chemistry dynamics and carbon dioxide fluxes across the atmosphere-ice-water interfaces in the Arctic Ocean: Pacific sector of the Arctic, *J. Mar. Syst.*, *66*(1), 204–226.

Sievers, J., L. L. Sørensen, T. Papakyriakou, B. Else, M. K. Sejr, D. Haubjerg Søgaard, D. Barber, and S. Rysgaard (2015), Winter observations of CO_2 exchange between sea ice and the atmosphere in a coastal fjord environment, *Cryosphere*, *9*(4), 1701–1713, doi:10.5194/tc-9-1701-2015.

Sirevaag, A., S. D. L. Rosa, I. Fer, M. Nicolaus, M. Tjernström, and M. G. McPhee (2011), Mixing, heat fluxes and heat content evolution of the Arctic Ocean mixed layer, *Ocean Sci.*, *7*(3), 335–349, doi:10.5194/os-7-335-2011.

Smith, M., and J. Thomson (2016), Scaling observations of surface waves in the Beaufort Sea, *Elementa: Sci. Anthropocene*, *4*(1), 97, doi:10.12952/journal.elementa.000097.

Sørensen, L. L., B. Jensen, R. N. Glud, D. F. Mcginnis, M. K. Sejr, J. Sievers, D. H. Søgaard, J. L. Tison, and S. Rysgaard (2014), Parameterization of atmosphere-surface exchange of CO_2 over sea ice, *Cryosphere*, *8*(3), 853–866, doi:10.5194/tc-8-853-2014.

Sotiropoulou, G., et al. (2016), Atmospheric conditions during the Arctic Clouds in Summer Experiment (ACSE): Contrasting open-water and sea-ice surfaces during melt and freeze-up seasons, *J. Clim.*, *29*, 8721–8744, doi:10.1175/JCLI-D-16-0211.1.

Spreen, G., L. Kaleschke, and G. Heygster (2008), Sea ice remote sensing using AMSR-E 89-GHz channels, *J. Geophys. Res.*, *113*, C02S03, doi:10.1029/2005JC003384.

Strong, C., and I. G. Rigor (2013), Arctic marginal ice zone trending wider in summer and narrower in winter, *Geophys. Res. Lett.*, *40*, 4864–4868, doi:10.1002/grl.50928.

Sutherland, P., and W. K. Melville (2015), Field measurements of surface and near-surface turbulence in the presence of breaking waves, *J. Phys. Oceanogr.*, *45*(4), 943–965.

Takahashi, T., et al. (2009), Climatological mean and decadal change in surface ocean pCO_2, and net sea–air CO_2 flux over the global oceans, *Deep Sea Res., Part. II*, *56*(8), 554–577, doi:10.1016/j.dsr2.2008.12.009.

Thornton, B. F., M. C. Geibel, P. M. Crill, C. Humborg, and C. M. Mörth (2016), Methane fluxes from the sea to the atmosphere across the Siberian shelf seas, *Geophys. Res. Lett.*, *43*, 5869–5877, doi:10.1002/2016GL068977.

Tjernström, M., et al. (2015), Warm-air advection, air mass transformation and fog causes rapid ice melt, *Geophys. Res. Lett.*, *42*, 5594–5602, doi:10.1002/2015GL064373.

van Heuven, S., D. Pierrot, J. W. B. Rae, E. Lewis, and D. W. R. Wallace (2011), *MATLAB Program Developed for CO_2 System Calculations. ORNL/CDIAC-105b. Carbon Dioxide Information Analysis Center*, Oak Ridge Natl. Lab., U.S. Dep. of Energy, Oak Ridge, Tenn., doi:10.3334/CDIAC/otg.CO2SYS_MATLAB_v1.1.

Wanninkhof, R. (2014), Relationship between wind speed and gas exchange over the ocean revisited, *Limnol. Oceanogr. Meth.*, *12*(6), 351–362, doi:10.4319/lom.2014.12.351.

Wanninkhof, R., W. E. Asher, D. T. Ho, C. Sweeney, and W. R. McGillis (2009), Advances in quantifying air-sea gas exchange and environmental forcing, *Annu. Rev. Mar. Sci.*, *1*, 213–244, doi:10.1146/annurev.marine.010908.163742.

Weiss, R. (1974), Carbon dioxide in water and seawater: The solubility of a non-ideal gas, *Mar. Chem.*, *2*(3), 203–215, doi:10.1016/0304-4203(74)90015-2.

Yang, M., J. Prytherch, E. Kozlova, M. J. Yelland, D. Parenkat Mony, and T. G. Bell (2016), Comparison of two closed-path cavity-based spectrometers for measuring air-water CO_2 and CH_4 fluxes by eddy covariance, *Atmos. Meas. Tech.*, *9*(11), 5509–5522, doi:10.5194/amt-9-5509-2016.

Yelland, M. J., B. I. Moat, R. W. Pascal, and D. I. Berry (2002), CFD model estimates of the airflow distortion over research ships and the impact on momentum flux measurements, *J. Atmos. Ocean. Technol.*, *19*, 1477–1499, doi:10.1175/1520-0426(2002)019<1477:CMEOTA>2.0.CO;2.

Zemmelink, H. J., B. Delille, J. L. Tison, E. J. Hintsa, L. Houghton, and J. W. Dacey (2006), CO_2 deposition over the multi-year ice of the western Weddell Sea. *Geophys. Res. Lett.*, *33*, L13606, doi:10.1029/2006GL026320.

Zippel, S., and J. Thomson (2016), Air-sea interactions in the marginal ice zone, *Elementa: Sci. Anthropocene*, *4*(1), 95, doi:10.12952/journal.elementa.000095.